

RESEARCH PAPER

PRELIMINARY INVESTIGATION INTO MECHANICAL PROPERTIES AND MICROSTRUCTURAL BEHAVIOUR OF INCONEL ALLOY UNDER WELDED AND UNWELDED CONDITIONS

*Saurabh Dewangan¹, Sharath Narayanan¹, Gurbaaz Singh Gill¹, Utkarsh Chadha²*¹ Department of Mechanical Engineering, Manipal University Jaipur, Jaipur, Rajasthan, India, Pin-303007² Department of Materials Science and Engineering, Faculty of Applied Sciences and Engineering, School of Graduate Studies, University of Toronto, Toronto, Ontario ON, Canada*Corresponding author: gurbaaz.199402071@mu.jaipur.edu, tel.: 0141-3999100-838, Manipal university Jaipur, 303007, Jaipur, Rajasthan, India

Received: 20.12.2022

Accepted: 11.01.2023

ABSTRACT

This work focusses on analyzing mechanical properties and microscopic assessment into Inconel-718 plates in welded and unwelded conditions. Welding was performed by tungsten inert gas welding technique. Two mechanical tests such as tensile test and hardness were performed on both the types of plates to compare the properties of welded joint and unwelded plate. Although Inconel 718 possesses good weldability, the strength, ductility, and hardness of welded joint were reported lesser than these of Unwelded plate. The microstructural images revealed that metal carbides present in Inconel plate had reduced after welding. The ultimate tensile stress and elongation before breaking of welded joint were 16% and 72% lower than Unwelded plate. The fractography analysis of the ruptured part revealed that Unwelded plate possessed higher ductility than welded plate.

Keywords: 718-Inconel alloy; welding; Tensile test; Hardness; Microstructure; Fractography

INTRODUCTION

Nickel-based super alloy is widely being used in various industry. These super alloys have certain advanced properties which are required to provide strength to machine parts in aerospace, chemical, marine, and automobiles. Nickel-based alloys are also utilized because of their high chemical, mechanical and thermal stability. Due to possessing good strength and temperature resistance, approximately 50% machine parts including compressor casing, discs, and fan blades of turbojet engines are made by Inconel 718 [1]. The high-strength super alloy Inconel 718 (also known as Alloy 718) has a nickel-chrome basis that makes it corrosion-resistant, high pressure- and temperature-resistant up to 700°C. The substance contains trace quantities of Mo, Ti, Co, Al, Cu, Mn, Si, and others. This alloy mainly imparts Ni (45-55%), Cr (15-20%), Nb (4-5%), and a little amount of Ta (tantalum) [2]. This nickel alloy resists spalling, break off into fragments, during temperature fluctuations. This occurs due to the development of a strong and tight oxide scale on the surface. Although Inconel 718 may be manufactured using techniques like electric discharge machining (EDM), laser beam machining (LBM), and other methods where stresses are created during machining, it is a tough alloy to cut and has a wide variety of uses [3].

This alloy's distinctive microstructure, which is made up of precipitates, γ'' , γ' , δ , carbides, and a γ -matrix, contributes to its advanced characteristics. The γ -matrix, which has FCC crystal structure, possesses a mixture of alloying elements like Cr, Mo, and Fe in Ni. The metastable phase of Ni_3Nb , gamma double prime (γ''), features a tetragonal space-centered crystal structure. It is a phase which provides larger amount of strength to Inconel

718. It is usually 15-20% (by volume) of the total structure volume. Gamma double primes undergo a transformation to the stable phase when exposed to high temperatures over an extended period of time. The stable form of Ni_3Nb is recognized as δ -phase. It contains orthorhombic crystal structure. The high amount of δ -phase is not desirable until it precipitates at the grain boundaries. It acts as barrier for grain expansion and improves the mechanical characteristics. Due to the tiny volume of γ' phase in the microstructure of Inconel 718, it has a negligible impact on the alloy's characteristics. The change of the γ'' phase into the δ phase, which occurs at high temperatures (above 700°C) and after sufficiently lengthy exposure, establishes the maximum temperature limit for Inconel 718's working state [4, 5]. A number of research works have been carried out with Inconel 718 metal which includes the observation of fatigue strength, microstructure, welding, heat treating etc. Some of the previous literatures have been separately discussion in literature review section.

In this work, a comparative assessment between welded and unwelded Inconel 718 alloy plates has been carried out on the basis of tensile test and hardness test results. The changes in microscopic level have been observed through optical microscopy (OM) and field emission scanning electron microscope (FESEM).

LITERATURE REVIEW

Inconel alloy has been investigated under many physical conditions- like welded condition, additive manufactured, thin film, high temperature applications, etc. Some of the previous works have been discussed comprehensively. In a work, Inconel 625

alloy was manufactured by using wire-arc based additive manufacturing (WAAM). Based on that, microstructure and physical attributes of the fabricated product have been analysed. The bottom layer of the alloy contained primary cellular grains. With an increase in wire-arc speed, the hardness of the alloy was found to increase. Similarly, ultimate tensile strength and yield strength were also got improved by additive manufacturing [6]. In a work by White et al. (2017), Inconel 625 was manufactured by selective laser melting (SLM) and then heat treated. As a result, a fine dendritic microstructure with strong texture was formed due to rapid cooling of the layers. Moreover, the γ -matrix was enriched with high dislocation density and good microhardness [7]. The welded joint between Inconel 625 and 16Mo3 steel was analysed in a work. The analysis was mainly focused on microstructural changes and chemical stability of the joint after annealing. After annealing for 10 hours at 600 to 1000°C, a strong grain orientation was reported in the joint which further enhanced the hardness of the surface [8]. The influence of heat input during TIG welding of Inconel-718 on strength and microstructure of the joints have been analysed by Jose and Anand. It was noticed that the joints made by low heat input possessed higher strength. Also, there was a reduction in grain size with a decrement in heat input [3]. The mixture of three oxides i.e., Cr_2O_3 , FeO, and MoO_3 was used as flux in TIG welding of Inconel 718 superalloy to check the effect on weldability, pool temperature, bead geometry, and strength of the joint. strength. As compared to conventional TIG welding, the modified version of welding process has increased the penetration by nearly 200%. Also, the hardness and strength of the joint was reported as better than the conventional one [9]. Because of carrying high strength at elevated temperature, Inconel 800H is used in aerospace industries. The effect of TIG welding on 800H alloy has been investigated. Both, pre-heat treated, and post-heat-treated conditions gave a good mechanical property. Post-weld heat treatment has been proved as a successful approach in Inconel welding [10]. Levin et al. (1997) investigated the wrought Inconel-625 alloy's high strain rate deformation behaviour and room temperature erosion behaviour. The steady state erosion rate was assessed to ascertain erosion resistance. After the erosion testing, microhardness tests were conducted, and substantial plastic deformation was seen close to the eroded surfaces. The mechanical characteristics were evaluated in the presence of high strain rate at elevated temperatures of 400°C-600°C. The erosion resistance was connected with high strain rate toughness and microhardness at the degraded surfaces [11]. The qualities of the final material are influenced by the thermal history that the additive manufacturing process generates. Although there are correlations between the rate of solidification and the final microstructure, the solidification rate alone cannot predict the final microstructure and consequently mechanical characteristics. The goal of the work of Bennetta et al. (2018) is to establish a connection between the produced material's final ultimate tensile strength and the combined impacts of cooling time as well as solidification time. It was determined how the construction geometry and final tensile strength of the location of interest compared to its thermal histories. The cooling time had a reverse effect on the distance of the point of observation from the substrate. Additionally, a pattern was seen connecting higher surface temperatures and longer solidification times. Coarse microstructures were the results of long cooling and solidification duration, which may be the reason of the lower observed tensile strengths, according to optical microscope photographs of the build microstructure [12]. The work of Brynk et al. (2017) is focussed on assessment of fatigue crack growth rate and tensile tests into Inconel 718 fabricated by Selective Laser Melting method in original form and with Re-addition. The laser melting technique produces comb

like layer-by-layer formation. A portion of the sample underwent the typical heat treatment process intended for Inconel 718 alloy. On the tensile strength, yield strength, and elongation to fracture, the effects of sample size, orientation to the laser beam direction, and heat treatment were examined. Good results were obtained for both types of samples [13]. In a work, selective laser melting technique was used to fabricate Inconel 718 cylinders. The fabricated cylinder showed columnar grains and arrays of body centered tetragonal Ni3Nb oblate. Due to which the hardness and tensile strength of fabricated sample were found comparable with wrought alloy [14]. The elevated temperature properties of Inconel 625 were examined by Oliveira et al. (2019). Tensile tests were conducted with strain rates of 2×10^{-4} to $2 \times 10^{-3} \text{ s}^{-1}$ at temperatures ranging from ambient temperature to 1000 C. The creep experiments were conducted in a continuous load mode at temperatures between 600 and 700 °C and stresses between 500 and 600 MPa. For observing surface fractures, optical and scanning electron microscopes were utilised. The dynamic strain ageing effect was connected to the serrated stress-strain behaviours seen in the curves obtained between 200 and 700 C. As a function of test temperature, the yield strength and the elongation values exhibit aberrant behaviour. A specimen that was tensile tested at 500°C showed intergranular cracking, which can be ascribed to the carbides at the grain boundaries losing cohesiveness. The specimen's fracture surface revealed a prevalence of trans granular cracking with tear dimples that had a parabolic form during the 700°C tensile test [15]. The mechanical properties of fine-grained Inconel 718 ring, fabricated by forging method, was reported as high. The toughness is reached up to 100 J. Also, the maximum stress for 107 fatigue cycles is about 620 MPa [16]. Other than 718 grade, Inconel 625 was also investigated under various experimental conditions. In a work 718 and 625 were welded by laser beam and fracture toughness of the joint was calculated. Both the alloys had shown similar behavior in ductile crack growth analysis. The fusion zone and heat affected one had shown comparatively lower value of fracture toughness than that of base metal zone [5]. Inconel 625 was also used as a source rod of TIG welding of ductile cast iron. Also, an electrode with 97.6% Ni constituent was used in welding. As a result, it was found that carbide formation had been restricted through this approach. By subsequent heating at 900°C, all carbides were reported to get dissolved into ferrite matrix as graphite [17]. Inconel 625 was welded with 16Mo3 for nanoindentation analysis of welded layer and of the transition between these two metals. An improved nano-hardness and a reduced elastic modulus were reported at transition zone [18]. The residual stress formed at the welded joints of Inconel 625 alloy was studied through experimentation and simulation methods. Both the XRD technique and ANSYS numerical code showed a close relationship of results [19]. Inconel alloy had been successfully welded with titanium alloy by laser beam welding. A good amount of fatigue strength was observed in the welded joint of dissimilar metals. These types of joints are usually required in oil and gas industries [20].

MATERIAL AND METHODS

Three nos. of Inconel-718 plates of dimension 100×50×3 mm each were taken for further analysis. One plate was kept as it is i.e., in un-welded condition. Remaining two plates were welded in butt configuration by tungsten inert gas (TIG) welding technique. The voltage and current selection for welding were 25V and 110A respectively. A filler wire of 1.5 mm diameter was applied during welding. Direct current electrode negative configuration was used for welding. The inert gas atmosphere of argon ($\text{Ar} \approx 99\%$) gas was supplied during welding operation. Fig. 1 is showing the schematic of plate selection and welded

joint. After welding, two sets of plates were collected- (1) The plate with no welding and (2) The welded plate. The goal is to examine the strength, hardness, and microstructure of the welded plates so that a comparative assessment could be done with another plate which is in unwelded condition.

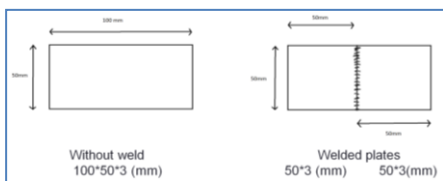


Fig. 1 Schematic of plate size selection for further processing

- **Fabrication of tension test specimen:** Both plates were cut with a wire EDM to produce specimens of the size required for tensile testing. The work produced test specifications according to the ASTM-E8 standard. The specimens are shown in Fig 2. The tensile test was conducted on Universal Testing Machine (UTM) with a strain rate of 0.00015 s⁻¹.



Fig. 2 Tensile test specimens- before and after tension test

- **Hardness test procedure:** The hardness of the specimen was measured through Brinell hardness tester. A common load of 187.5 kgf was applied on both the plates by using ball diameter of 2.5 mm. The cross-sectional surfaces of both the plates were finished properly so that unevenness could be avoided during indentation.
- **Microscopic analysis:** As a result of welding, the Inconel plate might have undergone through structural changes, it will be predicted by microstructural analysis through optical microscope. The cross-sectional surfaces of the specimens were used to observe the microstructural variation, if any. The desired surfaces were super finished by using various grades of sandpapers with grit sizes of 500, 100, 1500, 2000, and 2500. Superfinishing operation was done through a polishing machine. Finally, the polished surfaces were etched using HNO₃+HCl+H₂O₂+H₂O etchant, and then they were examined through optical microscope. The images were captured at 200× magnification.

RESULT ANALYSIS AND DISCUSSION

- **Tensile test results:** After conducting tensile test in both the samples, the stress-strain curves for the two specimens are provided in Fig. 3 (a, b). The dimensional details of specimens are also written in Fig. 3. The corresponding values of Ultimate tensile stress, yield stress and elongation values shown in Fig. 3 itself. As it can be seen from Fig, the ultimate tensile stress (UTS) and yield stress (YS) of Unwelded specimen are 894 MPa and 551 MPa respectively with 47% of elongation till failure.

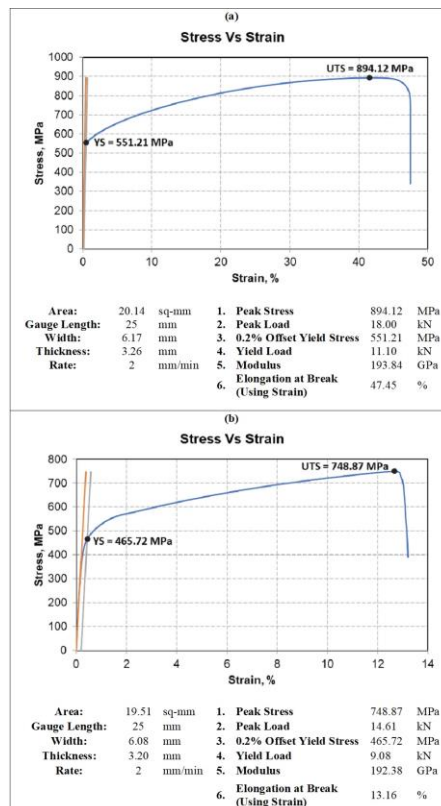


Fig. 3 Tensile test results of (a) Unwelded specimen; (b) Welded specimen.

The welded specimen showed UTS, and YS of 447 MPa, and 373 MPa respectively (Fig. 3b). These values are almost half of the Un-welded specimen. The elongation shown by welded specimen is 72% lower than that of un-welded specimen. The broken samples of both the specimens are quite different in appearance. The un-welded specimen showed a longer extension than welded one. There might be two possibilities of lesser strength and ductility of the welded joint: first, there is a huge possibility of welding defects in the welded joint which may cause a substantial reduction in strength as well as ductility. Second, the metal carbides (TiC) have disappeared in welded joint resulting in poor strength.

- **Hardness test results:** The results obtained by Brinell hardness test are given in Table 1.

Table 1 Hardness test results

Plates	Test value (BHN)
Un-welded	255
Welded	Base metal = 252, 240, 245 (Avg = 245)
	Heat affected zone = 251, 240, 256 (Avg = 249)
	Welded Joint = 237, 232, 230 (Avg = 233)

As per the results obtained, the hardness of unwelded specimen is 255 BHN. There are three different hardness values in welded plate. The hardness at parent (base) metal part, HAZ (heat affected zone) and fusion zone is 245, 249, 233 BHN respectively. The welded joint possesses almost 9% lesser hardness than Unwelded plate. The most probable reason behind the reduction in hardness might be improper mixing of the metal at fusion zone.

➤ **Microstructural test results:** As discussed above, the microscopic images were obtained by optical microscope. The model's name of the microscope is L-2003 A. The images for unwelded and welded plates are presented in Fig. 4 and Fig. 5 respectively. Mainly three different observations were made in this study. (1) γ -matrix; (2) MC carbide- a dark appearance in γ -matrix; (3) TiC boundaries (black in color). In both the images, the black colored TiC boundary could be properly seen. But the amount of MC carbides dispersed throughout the γ -matrix matrix is different. There is high amount of MC carbides in Unwelded plate whereas the welded joint imparts very less amount of it. This is the reason why the hardness of the unwelded plate becomes higher than the welded plate.

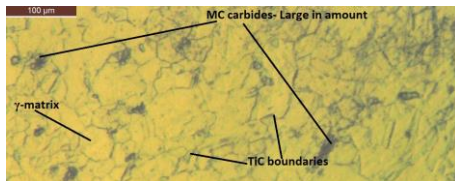


Fig. 4 Microstructure of Un-welded plate

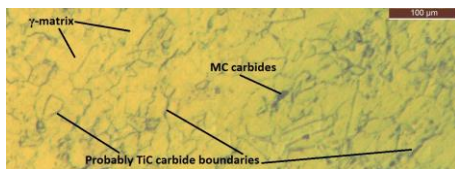


Fig. 5 Microstructure of Welded plate

➤ **Fractography analysis:** Fractographic examination was performed on the fractured tensile test samples. In order to determine the kind of failure—brittle or ductile—the specimen's broken surface was studied using FESEM. Unwelded and welded samples' fractographic images are depicted in Figs. 6 and 7, respectively. An enormous number of pores were found in the unwelded sample. Numerous micro-dimples are another sign of ductile fracture in addition to this. The welded sample has facets without noticeable pores, however certain micro-dimple zones have been observed. The fractography picture of the welded sample serves as evidence that the specimen is brittle in nature.

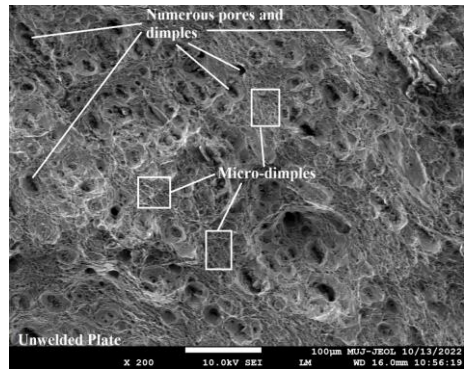


Fig. 6 Fractography image of unwelded specimen

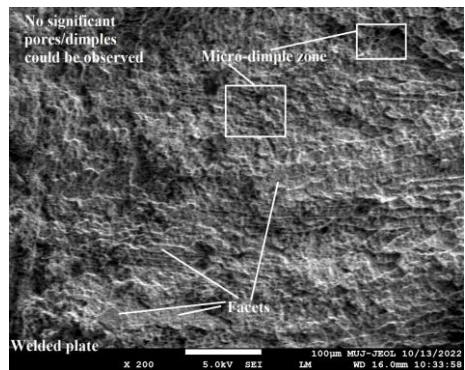


Fig. 7 Fractography image of welded specimen

DISCUSSION AND CONCLUSION

For making a good quality welded joint in any metal, the surface must be properly clean and finished otherwise the problem of impurity inclusion may happen in the fusion zone. Also, the cooling rate plays an important role in deciding the final properties of welded joint. The properties like tensile strength [21], hardness [22] and fatigue strength [23, 24] are highly affected by the cooling rate.

In this work, metallographic analysis of welded and Unwelded plates of Inconel alloy plates has been carried out. The following conclusion can be made based on experimental work:

- Inconel possesses a good weldability as far as similar metal joint is concerned.
- The Ultimate tensile strength of Inconel 718 alloy was reported as 894 MPa whereas the welded joint has showed a reduction of 16% in UTS.
- The yield stress of the welded joint (465.72 MPa) is comparable with unwelded specimen (551.21 MPa), although the joint has a reduction of 15% in yield stress.
- The elongation reported by welded sample is almost 72% lesser than unwelded one, means there is a high chance of poor welding with defects.
- Hardness values showed that unwelded plate has 9% higher hardness than welded plate.
- The Unwelded or pure plate was possessing high amount of MC carbides dispersed throughout the fine gamma-

matrix whereas lesser amount of MC carbide and TiC particles were reported in welded plate. It is the reason why hardness of the welded joint became less.

- Fractography analysis proves that unwelded specimen is more ductile than welded one because the latter one consists of facets with no considerable amounts of pores and dimples.

The present work has been conducted with a smaller number of samples. There might be possibilities of weld-defects in the fusion zone. Hence, a large number of samples can be taken to reach up to more accurate results.

REFERENCES

1. R. S. Silva, R. Demarque, L. M. Silva, J. A. Castro: *Soldagem & Inspeção*, 27, 2022, e2709. <https://doi.org/10.1590/0104-9224/SI27.09>.
2. Davis JR. Nickel, cobalt and their alloys. In: *Materials Park: ASM International*; 2000
3. P. J. Jose, M. D. Anand: *International Journal of Engineering & Technology*, 7, 2018, 206-209. <https://doi.org/10.14419/ijet.v7i3.6.14971>.
4. A. A. Popovich, V. Sh. Sufiiarov, I. A. Polozov, E. V. Borisov: *KEM*, 651–653, 2015, 665–670. <https://doi.org/10.4028/www.scientific.net/kem.651-653.665>.
5. C. Yeni, M. Kocak: *Fatigue & Fracture of Engineering Materials & Structures*, 29, 2006, 546-557. <https://doi.org/10.1111/j.1460-2695.2006.01025.x>.
6. W. Yangfan, C. Xizhang, S. Chuanchu: *Surface and Coatings Technology*, 374, 2019, 116-123. <https://doi.org/10.1016/j.surfcoat.2019.05.079>.
7. C. Li, R. White, X. Y. Fang, M. Weaver, Y. B. Guo: *Materials Science and Engineering A*, 705, 2017, 20-31. <https://doi.org/10.1016/j.msea.2017.08.058>.
8. P. Petrzak, K. Kowalski, M. Rozmus-Górnikowska, A. Dębowska, M. Jędrusik, D. Kocłęga: *Metallurgy and Foundry Engineering*, 44 (2), 2018, 73-80. <http://dx.doi.org/10.7494/mafe.2018.44.2.73>.
9. H. Kumar, G.N. Ahmad & N. K. Singh. *Materials and Manufacturing Processes*. 34(2), 2019, 216-223. <https://doi.org/10.1080/10426914.2018.1532581>.
10. A. Elmariung, S.M. Sivagami, C. Chanakyan, A. Joseph Arockiam, G.B. Sathishkumar, M. Meignanamoorthy, M. Ravichandran, S.V. Alagarsamy: *Materials Today: Proceedings*. <https://doi.org/10.1016/j.matpr.2021.01.049>.
11. B.F. Levin, K.S. Vecchio, J.N. DuPont, A. Marder: *Superalloys*, 1997, 479-488. https://www.tms.org/Superalloys/10.7449/1997/Superalloys_1997_479_488.pdf.
12. J. L. Bennetta, O. L. Kafka, H. Liao, S. J. Wolff, C. Yu, P. Cheng, G. Hyatt, K. Ehmann, J. Cao: *Procedia Manufacturing*, 26, 2018, 912-919. <https://doi.org/10.1016/j.promfg.2018.07.118>.
13. T. Brynk, Z. Pakiela, K. Ludwiewska, B. Romelczyk, R. M. Molak, M. Plocinsk, J. Kurzac, T. Kurzynowski, E. Chlebus: *Materials Science and Engineering: A*, 698, 2017, 289-301. <http://dx.doi.org/10.1016/j.msea.2017.05.052>.
14. K.N. Amato, S.M. Gaytan, L.E. Murr, E. Martinez, P.W. Shindo, J. Hernandez, S. Collins, F. Medina: *Acta Materialia*, 60(5), 2012, 2229-2239. <https://doi.org/10.1016/j.actamat.2011.12.032>.
15. M. M. de Oliveira, A. A. Couto, G. F. C. Almeida, D. A. P. Reis, N. B. de Lima, R. Baldan: *Metals* 9, 2019, 301. <https://doi.org/10.3390/met9030301>.
16. Z. Wang, D. Zhou, Q. Deng, G. Chen, W. Xie. The Microstructure and Mechanical Properties of Inconel 718 Fine Grain Ring Forging. In: *Superalloy 718 and Derivatives*, edited by: E.A. Ott, J.R. Groh, A. Banik, I. Dempster, T.P. Gabb, R. Helmink, X. Liu, A. Mitchell, G.P. Sjöberg, A. Wusatowska-Sarnek, Wiley Online 2010, 343-349. <https://doi.org/10.1002/9781118495223.ch26>.
17. F. J. CárcelCarrasco, M. A. PérezPuig, M. Pascual-Guilamón, R. Pascual-Martínez: *Metals*, 6, 2016, 283. <https://doi.org/10.3390/met6110283>.
18. P. Klučiar, I. Barený, J. Majerik: *Manufacturing Technology*, 22(1), 2022, 26-33. https://journalmt.com/artkey/mft-202201-0013_nanoindentation-analysis-of-inconel-625-alloy-weld-overlay-on-16mo3-steel.php.
19. H. Vemanaboina, E. Gundabattini, K. Kumar, P. Ferro, B. S. Babu: *Advances in Materials Science and Engineering*, 2021, Article ID 3948129, 2021, 12 pages. <https://doi.org/10.1155/2021/3948129>.
20. P. Corigliano, V. Crupi: *Ocean Engineering*, 221(1), 2021, 108582. <https://doi.org/10.1016/j.oceaneng.2021.108582>.
21. S. Dewangan, S.K. Selvaraj, T.M. Adane, S. Chattopadhyaya, G. Królczyk, R. Raju: *Advances in Materials Science and Engineering*, 2022. <https://doi.org/10.1155/2022/9377591>.
22. S. Dewangan, S. Chattopadhyaya: *Acta Metallurgica Slovaca*, 28(3), 2022, 140–146. <https://doi.org/10.36547/ams.28.3.1556>.
23. W. Macek, Z. Marciniak, R. Branco, D. Rozumek, G.M. Królczyk: *Measurement*, 178, 2021, Article Number: 109443. <https://doi.org/10.1016/j.measurement.2021.109443>.
24. W. Macek, D. Rozumek, G. M. Krolczyk: *Measurement*, 152, 2020, Article Number: 107347. <https://doi.org/10.1016/j.measurement.2019.107347>.